Detection of Neutral Particles in High Energy Experiments

Shinjiro Yasumi

KEK

Detection of neutral particles in high energy experiments

§1. Introduction

In high energy experiments, it is rather easy to measure a reaction when particles participating in the reaction are all charged. When some neutral particles are included in a reaction, however, it is necessary to measure the reaction more carefully.

Among various reactions in which some neutral particles are included, some charge exchange reactions such as $\pi^- + p \rightarrow \pi^\circ + n$, $\pi^- + p \rightarrow \eta + n$, and $K^- + p \rightarrow \overline{K}^\circ + n$, are important to be studied.

In these measurements the detection of neutral particles such as neutral pions, eta mesons and neutrons in necessary to be done. The accuracy of measurement of these reactions, sometimes, depends mainly upon the accuracy of neutral particle detection.

There are some reactions such as $\gamma + n \rightarrow \pi^\circ + n$ and $K^\circ_L \rightarrow 3\pi^\circ$, in which participating particles are all neutral. In order to investigate these reactions it is indispensable to detect, to identify and to measure neutral particles included in the reaction.

Since the detection of neutral particles is generally more complicated than that of charged particles, it is worth improving and developing a method and an apparatus for detecting neutral particles in hgih energy experiments.

Now I would like to give you a short lecture on the detection of neutral particles in high energy experiments, aiming at that you will be more familiar with this subject[1)] for the coming experiments using various beam lines from the KEK proton synchrotron in a few years from now.

§2. Classification of neutral particles from the viewpoint of the detection method.

In the case in which a neutral particle decays into some charged particles fastly enough to detect them with an "ordinary detecting system"* there seems to be little problem to detect and measure it. K_s°, Λ, and ρ, for example, are classified to this category as follows:

$$\left.\begin{array}{l} \pi^- + p \rightarrow K^\circ + \Lambda \\ K^\circ\ (K_s^\circ) \rightarrow \pi^- + \pi^+ \\ \Lambda \rightarrow \pi^- + p \end{array}\right\} \qquad (1)$$

$$\left.\begin{array}{l} \pi^- + p \rightarrow \rho^\circ + n \\ \rho^\circ \rightarrow \pi^- + \pi^+ \end{array}\right\} \qquad (2)$$

This kind of particles is referred to the category I.

On the other hand, in the case in which a neutral particle can pass through an ordinary detecting system without convering, it should be very careful to do with the neutral particle. This situation occurs, (a) if the life time of the neutral particle is long enough to cause such a situation, or (b) if particles decaying from the neutral particle are also neutral and their life times are long enough to pass through an ordinary detecting system.

Let us explain this point in giving some numbers. If we assume that the length of an ordinary detecting system D is, say, 10m, the passing time of a neutral particle through D with the light velocity is

$$T = \frac{D}{C} \sim 3 \times 10^{-8} \text{ sec}$$

---

* Here, an "ordinary detecting system" means the detecting system consisting of materials whose average radiation length and collision length are both nearly equal to those of air at the normal state.

Then a neutral particle whose life time is longer than 10^{-8} sec (roughly speaking!), can not be detected with the detecting system abovementioned. The kind of particles is referred to the category II- (a).

In the case in which, even if a neutral particle decays rather fastly, particles decaying from it are again neutral and also their life times are longer than 10^{-8} sec, then the original neutral particle can not be detected with an ordinary detecting system of 10 meters long. The kind of particles is referred to the category II - (b).

Table I shows a list of neutral particles calssified to the category II (including both II (a) and II (b)).

Table I

As you see in Table I, neutral particles whose life times are longer than 10^{-8} sec, are photons, neutrinos, K°_{L}'s and neutrons. For the examples of particles belonging to the category II (b), there are π° mesons, η mesons (2γ - decay mode), Σ° and Ξ°hyperons.

Taking their decay modes into account, the detection of all neutral particles belonging to the category II which we know so far, is evetually ascribable to the detection of five kinds of particles: the photon, the neutrino, the neutral pion, the eta meson and the neutron.

Table II

Table II shows you the interactions by which the neutral particles of the five kinds are converted into some charged particles and then they are detected. Among particles of five kinds, neutrinos, interact with matter only through the weak interaction. Since the detection of neutrinos requires detailed knowledge on the neutrino interactions with matter whose investigation is now in progress at various laboratories in the world, I shall leave this subject for the future.

Let me talk about the detection of neutrons, photons, neutral π mesons and eta mesons in §3, §4 and §5, respectively.

§3. Neutrons

In the low energy region, $B^{10}F_3$ proportional counter, which utilizes the resonance absorption phenomenon of low energy neutrons by a nucleus of boron 10. The cross section amounts to 3770 barns for thermal neutrons (0.025 eV). Usually this counter is used being embedded in some material for the slowing-down process (paraffin is mostly used for this purpose).

There is no resonance for the neutron interactions with matter in the high energy region. The cross section monotonously decreases with the energy and it seems to tend to some constant value.

Below 1 GeV, a plastic scintillation counter is very common to be used. Chemical composition of a plastic scintillator is approximately represented by the formula (CH)n. In a plastic scintillation counter, photons emitted along the path of charged particles in a scintillating material are detected with photomultipliers, which are produced in the neutron-proton scattering and in the reactions of (n, p), (n, n' 3α) and (n, n'γ) for a carbon nucleus. Since, even though the energy of an incident neutron is given, energies of charged particles produced in a scintillator have a continuous spectrum, one cannot determine the energy of an incident neutron from the information of the pulse height of counters, but it can be usually measured with the time of flight measurement. Good time resolution of the plastic scintillation counter enables us to measure the time when a neutron strikes a scintillation counter in an accuracy of 1×10^{-9}sec (1 n sec).

If one can know the time when the neutron was produced at some place, the time of flight between these two places gives its velocity (in other words, its momentum or energy).

The detection efficiency of a plastic scintillation counter for neutrons depends upon the bias voltage of electronic circuits used. Measured values of the detection efficiency of the plastic scintillation counter are given in Fig. 1 for three cases (Case 1, 2 and 3). In case 1[3], the bias voltage was set at 6 MeV in terms of the proton kinetic energy and a thickness of a scintillator was 28.6 cm. In case 2[4] and case 3[4], the bias levels were set at 10 MeV and 20 MeV in terms of the proton kinetic energy, respectively. In both cases a scintillator of 20 cm thick was used. In the figure, the solid curve represents the calculated values basing on the measured cross sections for the nuclear reactions relevant to the conversion to charged particles. The agreement between the measured and calculated values is good.

Fig. 1

It can be seen from Fig. 1, that the detection efficiency of usual plastic scintillation counter for neutrons at high energies is about 1 percent for 1 cm thickness of a scintillator at the bias level of 10 MeV in terms of the proton kinetic energy.

A neutron counter hodoscope which consists of a number of neutron counter modules gives us the information on the direction of flight of a neutron. Without using such a hodoscope, the device such as that of Bollini et al[5] can give the information of the impact point of neutrons. The method of this device utilizes the fact that the difference of the arrival time of photons, produced at the impact position of neutrons, to both ends of a long scintillator depends upon the impact point of neutrons. Bollini et al[5] measured the impact point of neutrons in an accuracy of 5 cm with the apparatus as schematically shown in Fig. 2, in which a plastic scintillator of 1 m long was used. Using this device, they obtained a mass spectrum on the bosons B° produced in the $\pi^- + p \rightarrow n + B°$ by measuring the energy spectrum of neutrons.

Fig. 2

In high energy region above 1 GeV, it becomes difficult to discriminate between neutrons and photons by measuring their flight times, because the velocity of neutrons having such a high energy gets near the light velocity. Therefore, a "nuclear reaction star" detector, so to speak, is used for detecting very high energy neutrons.

This device consists of a number of spark chambers (or scintillation counters) interspersed with thick metal plates, (iron plates are usually used for this purpose) by which a nuclear star initiated by high energy neutrons in the apparatus is detected. Since the collision length and the radiation length for iron are 12.8 cm and 1.8 cm, respectively, so a nuclear star initiated by high energy neutrons can be easily distinguished from an electromagnetic cascade shower initiated by high energy photons.

Gibbard et al[6)] used this kind of device as the neutron detector in their experiment of the neutron-proton elastic scattering from 8 to 30 GeV/c. Fig. 3 shows the experimental arrangement they used schematically.

Fig. 3

In their experiment they measured only the direction of scattered neutrons using the neutron detector.

Ringia et al[7)] also used a similar detector in their measurement on the differential cross sections for the small angle neutron-proton and neutron-nucleus elastic scattering at 4.8 GeV/c. Their neutron detector consisted of the combination of an iron conversion plate followed by an scintillation counter hodoscopes for X-Y coordinates and an ionization calorimeter. They measured both the impact position and the energy of scattered neutrons with the former and the latter, respectively.

§4. Photons

For the detection of high energy photons, a pair spectrometer provides the most accurate measurement on their energies. Typical energy resolution of a pair spectometer amounts to about 1 %.

However, its acceptance solid angle and detection efficiency are both rather small. Furthermore, the apparatus of this kind needs a huge magnet for detecting high energy photons, because the weight of a necessary magnet increases as the cube of the energy of photons[8]. Therefore the pair spectrometer seems to be not so suitable to high energy experiments.

On the other hand, there is a variety of photon detectors utilizing the phenomenon of the cascade shower[9]; for instance, Cerenkov counters of total absorption type, scintillation counters of total absorption type, shower detectors of sandwich type, and track delineating shower detectors. There are two types of shower detectors of sandwich type, one of which utilizing the Cerenkov light, and the other utilizing the scintillation light.

These detectors are more fit to high energy experiemnts than a pair spectrometer.

The best energy resolutions so far achieved with such kind of detectors are 2 % (FWHM) at 4 GeV and 1.2 % at 14 GeV. These are obtianed with a Na I scintillation counter of total absorption type by Hofstadter and his collaborators[10]. This kind of detector, however, is too sensitive to background radiations in an experimental area and also its time resolution is not so good.

A lead glass Cerenkov counter of total absorption type is widely used in high energy experiments, because of the excellent time resolution and the moderate energy resolution in addition to the ability of suppression of sensitivity for low energy background radiations. Typical energy resolutions easily obtianed with a lead glass Cerenkov counter of total absorption type are 20 ~ 30 % (FWHM) at 200 MeV and 10 ~ 15 % (FWHM) at 1 GeV.[9, 11, 12, 13] Its excellent time resolution enables us to use it as an element of the fast counting system. A track delineating shower detector is quite useful to measure the impact point of photons very accurately. I shall give you some examples of this use in connection with the measurement on neutral pi mesons and eta mesons in §5.

Finally I will show you Fig. 4, which gives you an idea on the recent status of photon detector performances. This figure is based on the papers of references 11, 12, 13, 14 and 15.

Fig. 4

Here I do not want to enter into the details but refer you to these original papers and some review articles[16].

§5. Neutral pions and eta mesons

As is shown in Table I, neutral pions and eta mesons decay into two photons shortly after they are produced. Although eta mesons have the other decay modes in which they decay into three particles, usually the decay mode into two photons is used to detect and identify the eta mesons[17].

To identify π° and η mesons and to measure their momentum vectors, two decay photons are measured by using two systems of photon detectors as described in §4.

Let me explain how to measure π° mesons. For η mesons, the same method as that for π° mesons can be applicable. Fig. 5 gives a schematic diagram of the decay of a π° meson into two photons. The decay kinematics tells us the following relations:

$$E\pi^\circ = k_1 + k_2 \qquad (3)$$

$$k_1 \cdot k_2 = \mu^2 / 2(1-\cos\phi) \qquad (4)$$

$$k_2/k_1 = \sin\theta_1 / \sin(\phi - \phi_1) \qquad (5)$$

where

$E\pi^\circ$: Total energy of a π° meson.

μ : rest mass of a π° meson.

k_1, k_2 : energies of two photons decaying from a π° meson.

θ_1, θ_2 : angles between the directions of a π° meson and each photon decaying from a ° meson.

ϕ : correlation angle between the directions of two decay photons.

The correlation angle ϕ has the minimum value expressed by the following relation;

$$\phi\text{min} = 2 \arcsin(\mu/E_{\pi^\circ}) \qquad (6)$$

It follows from Eq. (6) that the minimum correlation angle decreases with the energy of a pion.

Among the quantities appearing in equations (3) ~ (5), ϕ, k_1 and k_2 are measurable. If you measure these three quantities, you can get a momentum vector of a π° meson by using the method as described in the last part of this section.

Generally speaking, it is not so easy to measure the energy of photons within an accuracy of a few percent as mentioned in §4. The direction of photons, however, can be measured more accurately. Using some devices as is schematically drawn in (a), (b) and (d) of Fig. 6, the impact point of a photon can be determined in an accuracy of a few millimeters. In these experimental arrangements you have to make a compromise between the detection efficiency and the angular and energy resolution by choosing the appropriate thickness of converters. Usually a lead plate of 1 to 2 radiation lengths in total is used for the conversion foil. A device as shown in (a) of Fig. 6

Fig. 6 (a), (b), (c) & (d)

---

enables us to make more accurate measurement of the impact point of photons than a device in (b) of Fig. 6 even if a counter hodoscope is replaced by spark chambers, for a converter of the same thickness. Because in the device of (a), many thin conversion foils are interspersed between spark (or wire) chambers, and so an accuracy of determining the impact point of photons is less suffered from the struggling of shower electrons inside a converter.

In a device as shown in (c) of Fig. 6, the energy resolution obtained with a Cerenkov counter of total absorption type is not so deteriorated by the preceding materials, but an accuracy of determining the impact point of photons amounts to at most, a few centimeters mainly due to the extent of shower development and the finite size of a module of Cerenkov counters.

An arrangement as shown in (d) of Fig. 6 enables us to make some over - determination measurements, thus improving very much an accuracy of tracking a photon - initiated electromagnetic cascade shower[14, 18].

The accuracy in measuring the correlation angle ϕ is much better than that in measuring energies of two decay photons. Therefore the quantity of the right hand side of equation (4) can be measured with much better precision as compared that of the left hand side of it.

Fig. 7

A hyperbola in the $k_1 - k_2$ diagram of Fig. 7 represents the equation (2) basing on the measured value of the correlation angle ϕ. A point (k_1', k_2') which corresponds to the measured values of energies of two decay photons, should be on the hyperbola. However, the point (k_1', k_2') does not always fall on the hyperbola, because of mainly the poor energy resolution of Cerenkov counters (or the other photon detectors). Deviations of the point (k_1', k_2') from the hyperbola is considered to be proportional to the experimental errors in measuring energies, Δk. The point at which an ellipse whose center is the point (k_1', k_2') and whose long and short radii are proportional to Δk_1 and Δk_2, respectively, osculates with the hyperbola, is considered to be the point corresponding to the most probable photon energies, say (k_1'', k_2'').

Knowing the energies (k_1'', k_2'') and the directions of two decay photons from the π° meson, the energy and direction (in other words, the momentum vector) of the π° meson can be obtained from the energy-momentum conversion law.

In the experiments on the $\gamma+p \rightarrow \pi^\circ+p$ and $\gamma+n \rightarrow \pi^\circ+n$ reactions,[4, 20, 21] Kyoto University's group measured π° mesons using the method above-mentioned in which they assumed Δk_1 equals to Δk_2, in other words, the error Δk was assumed to be constant, namely, to be independent of the energy. In this case, the ellipse just mentioned above becomes a circule[19].

In the experiment on the $\gamma+p \to \eta+p$ reaction Booth et al[22] measured neutral pions using the same method in which k was assumed to be proportional to k. This corresponds to that the most probable values (k_1', k_2') they adopted is the intersecting point between the hyperbola and the straight line joining the origin of the coordinate system and the point (k_1', k_2').

Thus the energy of $\pi°$ mesons can be measured with an accuracy of 4 ~ 5 % (FWHM) in the energy region from 0.3 GeV to 2 GeV, even though the energy resolution of photon detectors usually amounts to 20 ~ 30 % (FWHM).

In most high energy experiments, the total energy of the reaction system is known from the initial condition. When neutral pions on eta mesons are produced in some two body reaction whose reaction energy is known, the energy of $\pi°$ mesons to be measured can be easily estimated by the kinematics.

In order to detect and identify a $\pi°$ meson in such a case, we need only the correlation angle measurement on two decay photons from the $\pi°$ meson.

Table III gives several examples of measurements of neutral pions and eta mesons.

Table III

Here I would like to remind you that among the experiments listed in Table III, the experiment of the $\gamma+n \to \pi°+n$ reaction is one of the most difficult ones, because 1) all particles participating in this reaction are neutral, 2) the incident photon beam has a continuous spectrum due to the bremsstrahlung, and 3) the target neutron is moving in all directions due to the Fermi motion in a deuteron nucleus.

In the $\gamma+n \to \pi°+n$ reaction in the energy region between 0.5 and 0.9 GeV, the validity of the spectator model was verified by Kyoto University Group[4, 21].

In order to investigate the above-mentioned reaction in detail, we have to measure all kinematic quantities of both the π° meson and the neutron in the final state. In other words, we have to reconstruct the initial state of the reaction for each event from the quantities on the final state, in which there is only one constraint, that is, a given direction of the incident photon beam. Kyoto University's group performed, as the matter of fact, the first accurate measurements on the differential cross section of the $\gamma + n \to \pi^{\circ} + n$ reaction in the energy region between 500 MeV and 900 MeV[4, 21, 27, 28] by applying the method as described in this section for the detection of π° mesons. In such a case the method of determining the momentum vector of π° mesons was quite efficiently used. I do not want enter into the details here, but I would like to refer you to the original papers.

References

1) S. Yasumi and K. Miyake: Butsuri, 27(1972) 896 (in Japanese).

2) Particle Data Group: Rev. Mod. Phys. 45. No. 2, Pt. II (1973) S 15.

3) D.E. Crabb et al : Nuclear Instrum. and Methods, 48(1967) 87.

4) Y. Hemmi, T. Inagaki, R. Kikuchi, A. Maki, K. Miyake, T. Nakamura, A. Sasaki, N. Tamura, S. Yasumi and H. Okuno: Phys. Letters, 32B(1970) 137.

5) D. Bollini et al : Nuovo Cimento, 61A(1969) 125.

6) B.G. Gibbard et al : Phys. Rev. Letters, 24(1970) 22.

7) F.E. Ringia et al : Phys. Rev. Letters, 28(1972) 185.

8) A. Kantz and R. Hofstadter: Nucleonics, 12(1954) 36.

9) S. Yasumi: Butsuri, 25(1970) 571 (in Japanese).

10) R. Hofstadter, E.B. Hughes, W.L. Lakin and I. Sick: Nature, 221(1969) 228.

11) D. Luckey: Proc. Intern'l Symp. on Electron and Photon Interactions (Hamburg, 1965) Vol. II. p. 397.

12) Y. Hemmi, R. Kikuchi, S. Kobayashi, K. Miyake, T. Nakamura, H. Okuno, S. Yasumi and Y. Yoshimura: Nuclear Instrum. and Methods, 56(1967) 213.

13) M. Hayashi, S. Homma, N. Kajiura, T. Kondo and S. Yamada: Nuclear Instrum. and Methods, 94(1971) 297.

14) M. Holder, E. Radermacher, A. Staude, P. Darriulat, J. Deutsch, J. Pilcher, C. Rubbia, K. Tittel, C. Grosso-Pilcher, M. Scire and A. Villari: Nuclear Instrum. and Methods, 108(1973) 541.

15) E.B. Hughes and R. Hofstadter: HELP Report, 631(1970).

16) For instance, reference 9).

17) M. Chretien et al : Phys. Rev. Letters, 9(1962) 127.

18) M. Holder, E. Radermacher, A. Staude, P. Darriulat, J. Deutsch, M. Hansroul, S. Orito, J. Pilcher, C. Rubbia, P. Strolin, K. Tittel, A. Fainberg, C. Grosso-Pilcher and M. Scire: Phys. Letters, 40B(1972) 141.

19) L. Tau: Nuclear Instrum. and Methods, 34(1965) 352.

20) Y. Hemmi, T. Inagaki, Y. Inagaki, A. Maki, K. Miyake, T. Nakamura, N. Tamura, J. Tsukamoto, N. Yamashita, H. Itoh, S. Kobayashi, S. Yasumi and H. Yoshida: Phys. Letters, 43B(1973) 79.

21) Y. Hemmi, T. Inagaki, R. Kikuchi, A. Maki, K, Miyake, T. Nakamura, A. Sasaki, N. Tamura, S. Yasumi and H. Okuno: Nucl. Phys. B55(1973) 333.

22) P.S.L. Booth et al : Lettere al Nuovo Cimento, 2(1969) 66.

23) P. Borgeaud et al : Phys. Letters, 10(1964) 134.

24) A.V. Stirling et al : Phys. Rev. Letters, 14(1965) 763.

25) M.A. Wahlig et al : Phys. Rev. Letters, 13(1964) 103.

26) I. Mannelli et al : Phys. Rev. Letters, 14(1965) 408.

27) Y. Hemmi: Memoirs of the Faculty of Science, Kyoto University, Ser. A of Physics, Astrophysics, Geophysics and Chemistry, 33(1971) 339.

28) H. Okuno: ibid., 34(1972) 61.

Table I

Neutral particles classified to the category II. (For the definition of the category II, see the text)
Properties of particles in this table is based on Tables of Particles of 1973[2]. Partial decay modes having a fraction of less than 1 % are motted in this talk.

Particle	mean life (sec) $c\tau$ (cm)	Partial decay mode: Mode	Fraction (%)
photon (γ)	stable		
neutrino (ν) $\{\nu_e, \nu_\mu\}$	stable		
π°	0.84×10^{16}	$\gamma\ \gamma$	98.83 ± 0.05
	$\pm.10$	$\gamma e^+ e^-$	1.17 ± 0.05
	$c\tau = 2.5 \times 10^{-6}$		
K_L°		$\pi^\circ\pi^\circ\pi^\circ$	21.5 ± 0.8
	5.181×10^{-8}	$\pi^+\pi^-\pi^\circ$	12.6 ± 0.3
	$\pm.041$	$\pi\ \mu\ \nu$	26.9 ± 0.6
	$c\tau = 1553$	$\pi\ e\ \nu$	38.8 ± 0.6
		$\pi\ e\ \nu\ \gamma$	1.3 ± 0.8
η	$\Gamma = (2.63 \pm 0.58)$KeV	Neutral decays 71.1 %: $\gamma\ \gamma$	38.0 ± 1.0
		$\pi^\circ\gamma\ \gamma$	3.1 ± 1.1
		$3\pi^\circ$	30.0 ± 1.1
		Charged decays 28.9 %: $\pi^+\pi^-\pi^\circ$	23.9 ± 0.6
		$\pi^+\pi^-\gamma$	5.0 ± 0.1
n	$(0.918 \quad 0.014)10^3$	$p\ e^-\ \nu$	100
	$c\tau = 2.75 \times 10^{13}$		
Σ°	$<1.0 \times 10^{-14}$	$\Lambda\ \gamma$	100
Ξ°	2.98×10^{-10}		
	$\pm.12$	$\Lambda\pi^\circ$	100
	$c\tau = 8.93$		

Table II

Interactions by which the five kinds of neutral particles mentioned in the text, are converted into charged particles and thus detected.

Particle	Interaction
photon	electromagnetic interaction
neutrino	weak interaction
π° meson	electromagnetic interaction
η meson (2 γ decay)	electromagnetic interaction
neutron	strong interaction

Table III   Some examples of measurements of neutral pions and eta mesons

Reaction	Detector	Resolution: Energy	Resolution: Angle	Measured quantity	Reference
$\pi^- + p \to \pi^\circ + n$ at 0.8~1.9 GeV[23] $\theta_{\pi}^{cm} \sim 0^\circ$ at 6 18~GeV[24]	spark chamber		~4°	ϕ and k_1/k_2 ratio	(23) and (24)
$\pi^- + p \to \pi^\circ + n$ at 2.4~6.0 GeV[25] $\theta_{\pi^\circ}^{cm} \sim 0^\circ$ at 6~18 GeV[26]	spark chamber		0°~4.6°	ϕ	(25) and (26)
$\gamma + p \to \eta + p$ at 1.2~1.85 GeV $\theta_{\eta}^{cm} \sim 0^\circ$	spark chamber and Čerenkov counter of total absorption type	5~10 %	3°~9°	ϕ, k_1 and k_2	(22)
$\gamma + n \to \pi^\circ + n$ at 0.5~0.9 GeV $45^\circ < \theta_{\pi^\circ}^{cm} < 140^\circ$	spark chamber and Cerenkov counter of total absorption type	3~6%	3°	ϕ, k_1 and k_2	(4) and (21)
$\gamma + p \to \pi^\circ + p$ at 0.3~1.2 GeV $\theta_{\pi^\circ}^{cm} \sim 0$	scintillation counter hodoscope and Čerenkov counter of total absorption type	4~7%	2°~7°	ϕ, k_1 and k_2	(20)
$K_L \to \pi^\circ \pi^\circ$	spark chamber and Čerenkov counter hodoscope of total absorption type	The resultant precision in the vertex reconstruction $\sim\frac{1}{5}$ Ks lifetimes in the longitudinal direction		ϕ, k_1 and k_2	(18)

Figure captions

Fig. 1 Detection efficiency of a plastic scintillation counter for neutrons[1, 3, 4)]

For case 1, 2 and 3, see the text.

Fig. 2 Measurement on the impact point of neutrons[1, 5)]

When a neutron is incident upon a point C and converted into some charged particles there, the difference of the arrival times of photons produced at C to two ends of a long scintillator AB is proportional to $|\overline{AC}-\overline{CB}|$.

Fig. 3 Experimental setup for the neutron-proton elastic scattering from 8 to 30 GeV/c by Gilbard et al[1, 6)].

This figure is schematically drawn, where

Fe SC 1-7: iron spark chamber of 4 layers

A-SC : thin plate "anti" spark chamber

A : anti counter

S1-S7 : plastic scintillation counter

SC1-SC4 : thin plate spark chamber for the proton detection[11~15)]

Fig. 4 Performance of various kinds of photon detectors (Energy resolution VS Energy Curves)

Fig. 5 Diagram of the π° (or η) decay into two photons[1)]

Fig. 6 Measurement on the energy and the impact point of photons using various devices schematically drawn in (a) ~ (d)

A : anti counter

LSC: lead spark chamber (A lead spark chamber means a device in which lead converter foils are interspersed between spark chambers).

C : Cerenkov counter of total absorption type

C : lead converter

H : counter hodoscope

For detail, refer to the text.

Fig. 7 Method of determining the momentum vector of π° (or η) mesons[1)].

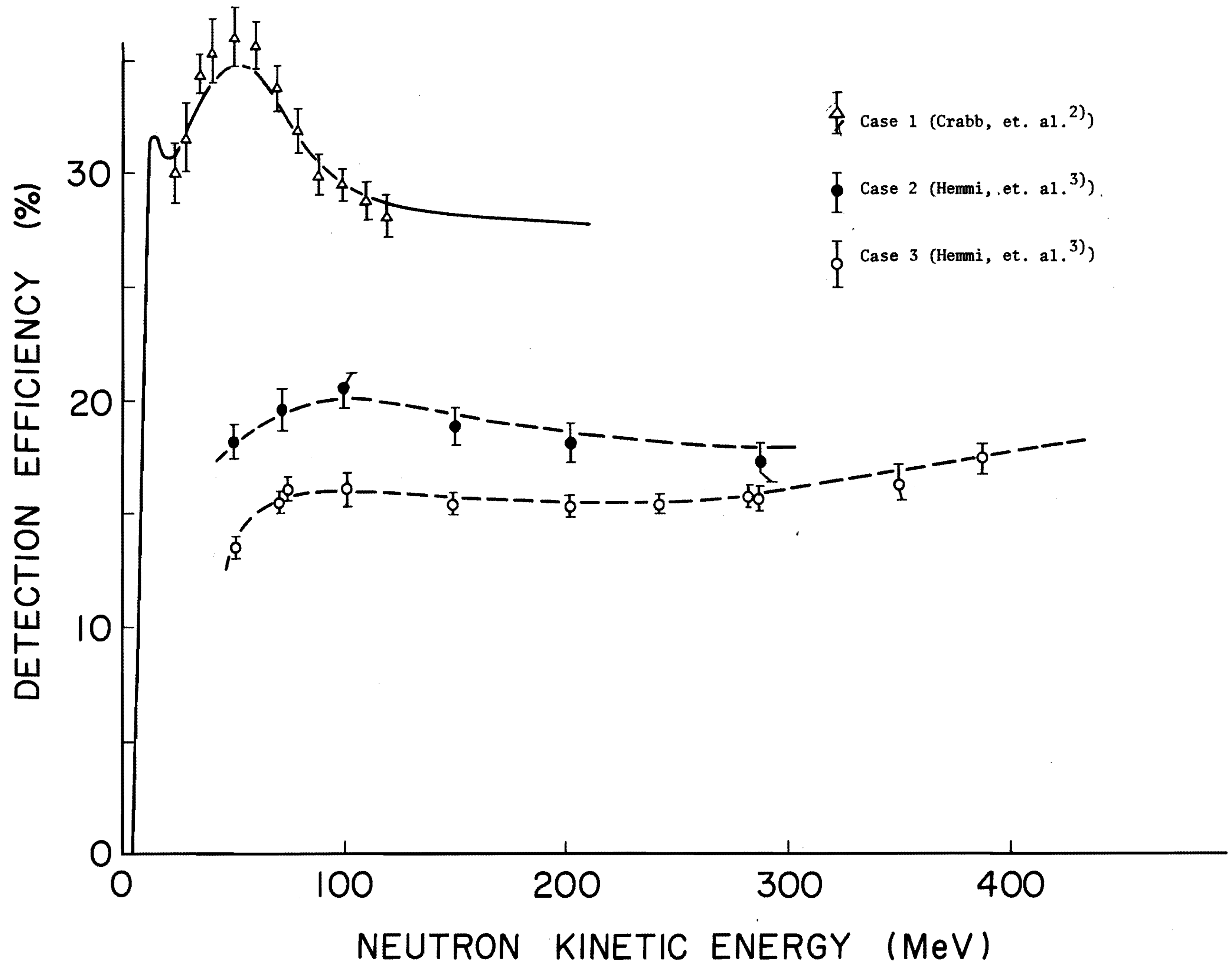
Case 1 (Crabb, et. al.2))
Case 2 (Hemmi, et. al.3))
Case 3 (Hemmi, et. al.3))
DETECTION EFFICIENCY (%)
NEUTRON KINETIC ENERGY (MeV)
0
10
20
30
0
100
200
300
400

(Fig. 1)

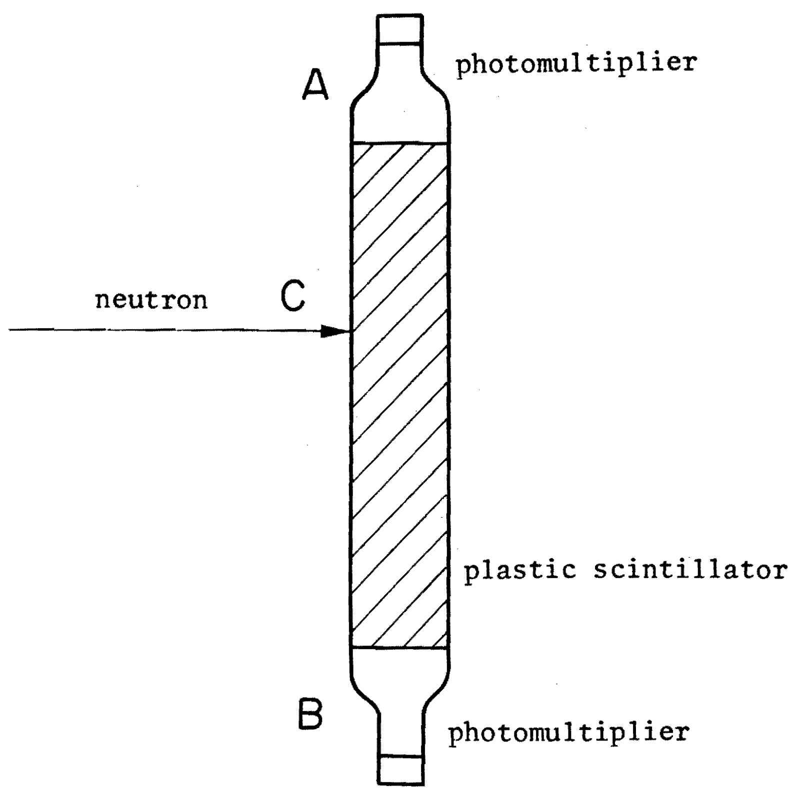
photomultiplier
A
neutron
C
plastic scintillator
B
photomultiplier

(Fig. 2)

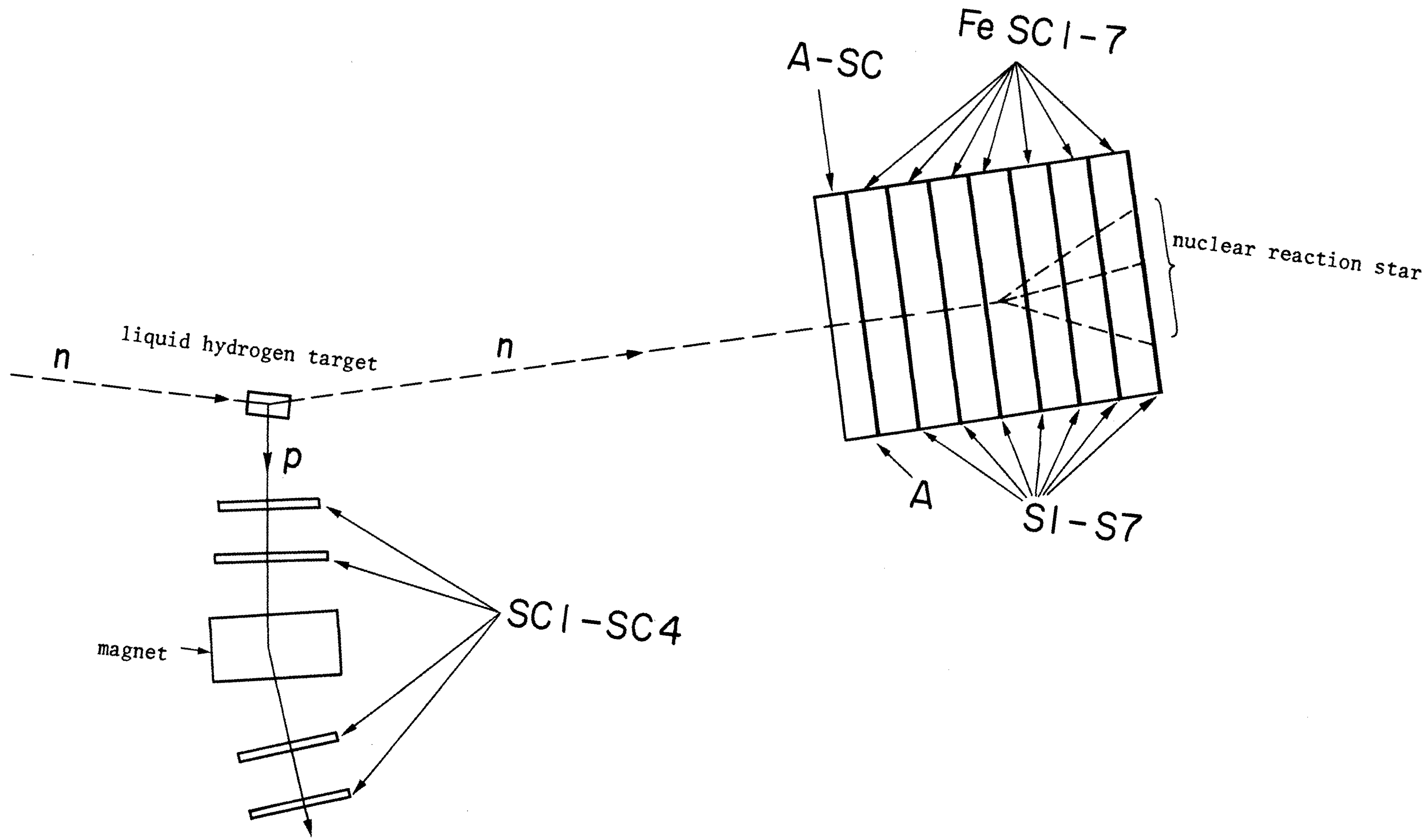
A-SC
Fe SC1-7
nuclear reaction star
n
liquid hydrogen target
n
p
A
S1-S7
SC1-SC4
magnet

(Fig. 3)

(Fig. 4)

Energy resolution vs Energy

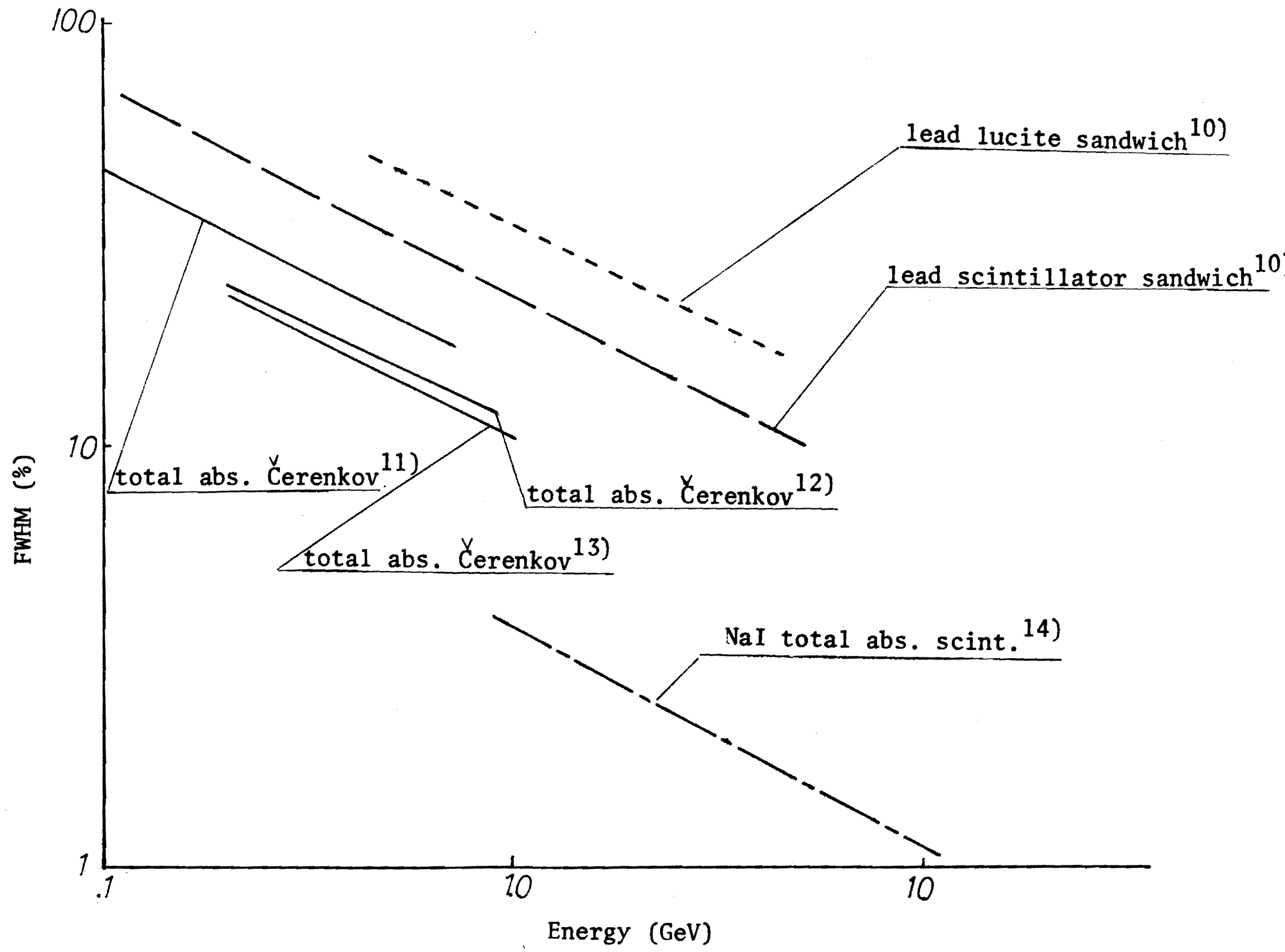

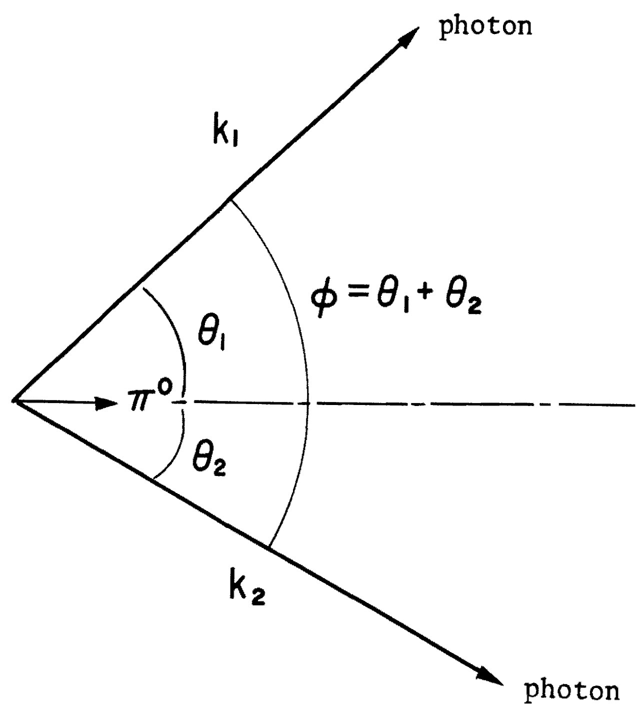
photon
k_1
$\phi = \theta_1 + \theta_2$
θ_1
π^0
θ_2
k_2
photon

(Fig. 5)

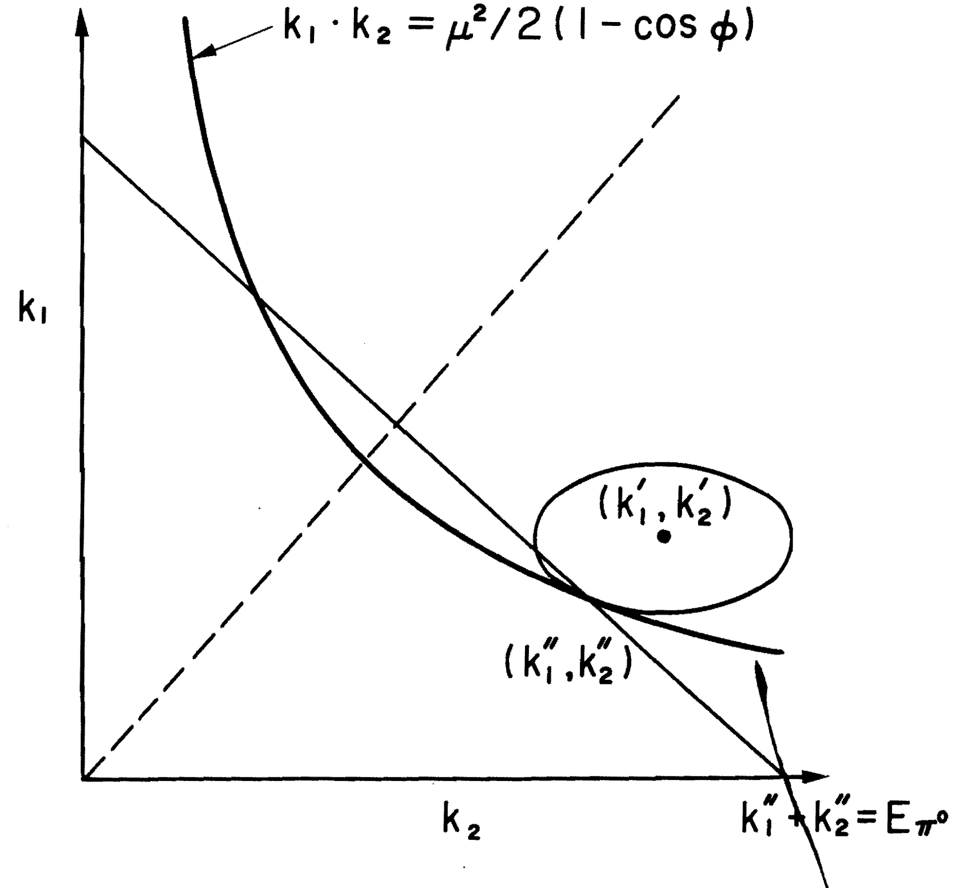
$k_1 \cdot k_2 = \mu^2/2(1-\cos\phi)$
k_1
(k_1', k_2')
(k_1'', k_2'')
k_2
$k_1'' + k_2'' = E_{\pi^0}$

(Fig. 7)

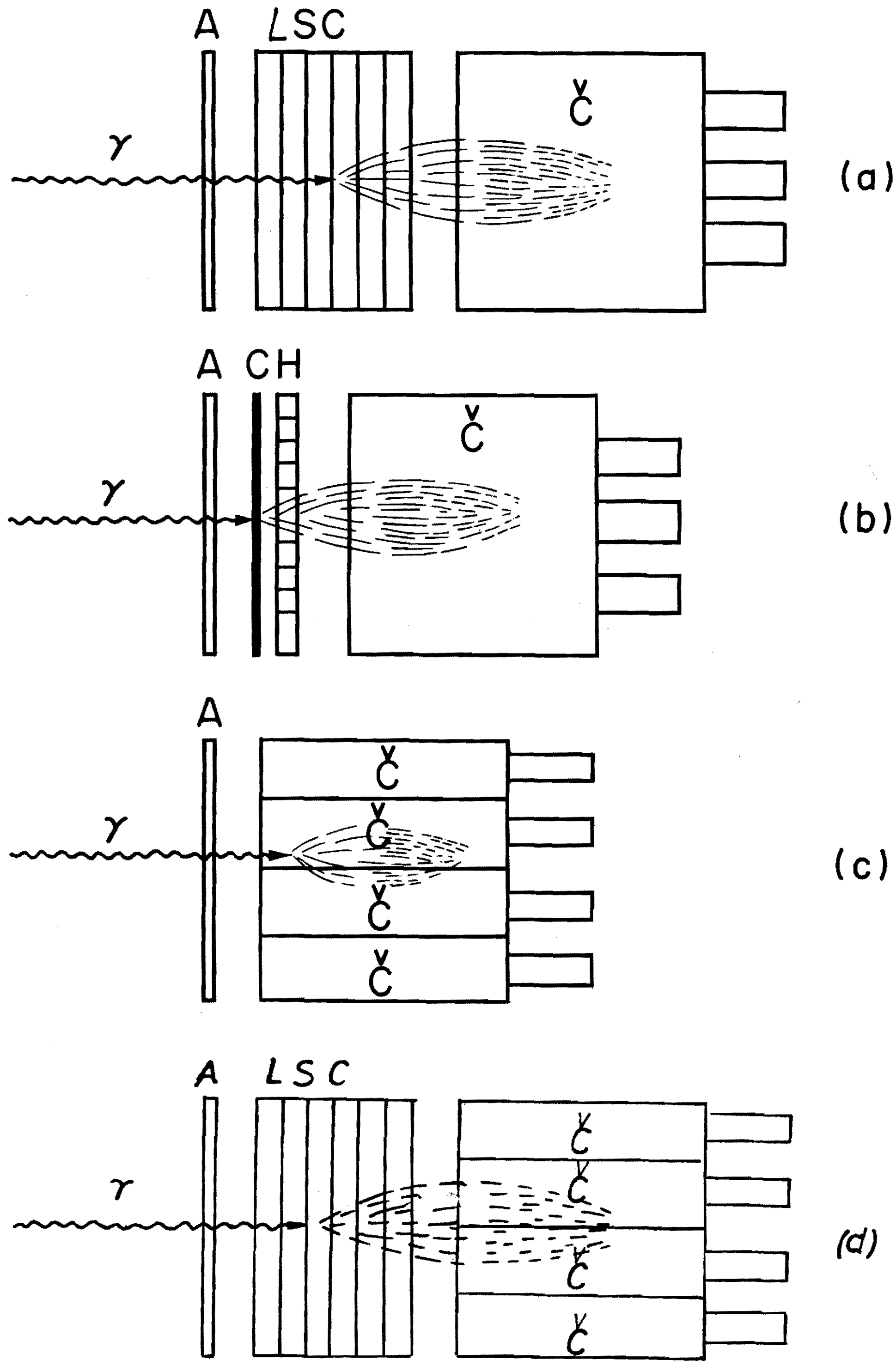

(Fig. 6)